

Structure and rotations of the Hoyle state

Evgeny Epelbaum^a, Hermann Krebs^a, Timo Lähde^b, Dean Lee^d, Ulf-G. Meißner^{e,b,c}

^a*Institut für Theoretische Physik II,*

Ruhr-Universität Bochum, D-44870 Bochum, Germany

^b*Institut für Kernphysik, Institute for Advanced Simulation,*

Jülich Center for Hadron Physics,

Forschungszentrum Jülich, D-52425 Jülich, Germany

^c*JARA - High Performance Computing,*

Forschungszentrum Jülich, D-52425 Jülich, Germany

^d*Department of Physics,*

North Carolina State University, Raleigh, NC 27695, USA

^e*Helmholtz-Institut für Strahlen- und Kernphysik and Bethe Center for Theoretical Physics,*

Universität Bonn, D-53115 Bonn, Germany

The Hoyle state is one of the most interesting and important challenges in nuclear physics. This excited state of the ^{12}C nucleus plays a key role in the fusion of three alpha particles to form carbon in red giant stars. In this letter we present *ab initio* lattice calculations which unravel the structure of this state and find evidence for a low-lying spin-2 rotational excitation. For the structure of the ^{12}C ground state and first spin-2 state, we find a compact triangular configuration of alpha clusters. For the Hoyle state and second spin-2 state, we find a bent-arm or obtuse triangular configuration of alpha clusters. We calculate electromagnetic transition rates among the various low-lying states.

PACS numbers: 21.10.Dr, 21.30.-x, 21.45-v, 21.60.De, 26.20.Fj

The carbon nucleus ^{12}C is produced by fusion of three alpha particles inside red giant stars. Without any resonant enhancement, however, the triple-alpha reaction rate is too low to explain the abundance of carbon in our universe. In the early 1950's, Öpik and Salpeter noted independently that the first step of merging two alpha particles is enhanced by the formation of ^8Be [1–3]. The ground state of ^8Be is a resonance with energy 92 keV above the ^4He - ^4He threshold with a width of 2.5 eV. A year later, however, Hoyle realized that this enhancement is still not enough to explain the observed carbon abundance. To resolve the discrepancy, Hoyle predicted a new positive-parity resonance of ^{12}C just above the combined masses of ^8Be and ^4He [4].

About three years later, Cook, Fowler, Lauritsen, and Lauritsen, experimentally observed a $J^\pi = 0^+$ state 278 keV above the ^8Be - ^4He threshold [5]. This 0_2^+ excited state has a width of 8.5 eV, and is now commonly known as the Hoyle state. The triple-alpha reaction is completed when the Hoyle state decays electromagnetically to the 2_1^+ state and then subsequently to the 0_1^+ ground state. Around the time of the experimental confirmation of the Hoyle state, Morinaga conjectured that the structure of excited alpha-nuclei such as the Hoyle state maybe be non-spherical [6]. This would imply low-lying even-parity rotational excitations. But there are also other ideas for the Hoyle state structure such as a diffuse trimer of alpha particles [7]. Recently the spin-2 Hoyle state has attracted considerable interest as the focus of several experimental investigations [8–12].

Recently we have presented an *ab initio* lattice calculation of the Hoyle state [13]. In that work the low-lying

spectrum of ^{12}C was calculated using the framework of chiral effective field theory and Monte Carlo lattice simulations. In this letter we continue these investigations and present *ab initio* lattice results that answer some questions about the structure of the Hoyle state and the existence of rotational excitations. We find evidence for a low-lying spin-2 rotational excitation of the Hoyle state. For the Hoyle state and its spin-2 excitation, we find strong overlap with a bent-arm or obtuse triangular configuration of alpha clusters. This is in contrast with the ^{12}C ground state and the first spin-2 state, where we see strong overlap with a compact triangular configuration of alpha clusters. We also calculate the electromagnetic transition rates among the low-lying even-parity states of ^{12}C . Our lattice results can be compared with other recent theoretical calculations for the low-lying spectrum of ^{12}C using the no-core shell model [14, 15] and variational calculations using Fermionic Molecular Dynamics [16, 17].

Chiral effective field theory treats the interactions of protons and neutrons as a systematic expansion in powers of nucleon momenta and the pion mass. A recent review can be found in Ref. [18]. The low-energy expansion is organized in powers of Q , where Q denotes the typical momentum of particles and is treated on the same footing as the mass of the pion. The most important contributions to the nuclear Hamiltonian come at leading order (LO) or $O(Q^0)$, while the next-to-leading order (NLO) terms are $O(Q^2)$. In the lattice calculations presented here, we include all possible interactions up to next-to-next-to-leading order (NNLO) or $O(Q^3)$.

In this analysis we use a periodic cubic lattice with lat-

tice spacing $a = 1.97$ fm and total length $L = 12$ fm. In the time direction, we use lattice time step $a_t = 1.32$ fm and vary the propagation time L_t to extrapolate to the limit $L_t \rightarrow \infty$. The nucleons are treated as point-like particles on lattice sites, and interactions due to the exchange of pions and multi-nucleon operators are generated using auxiliary fields. Lattice effective field theory was originally used to calculate the many-body properties of homogeneous nuclear and neutron matter [19, 20]. Since then the properties of several atomic nuclei have been investigated [21, 22]. A recent review of the literature can be found in Ref. [23].

Euclidean time propagation is used to project on to low-energy states of our interacting system. Let H be the Hamiltonian. For any initial quantum state Ψ , the projection amplitude is defined as the expectation value $\langle e^{-Ht} \rangle_\Psi$. For large Euclidean time t , the exponential operator e^{-Ht} enhances the signal of low-energy states. Energies can be determined from the exponential decay of these projection amplitudes. The first few time steps and last few time steps are evaluated using a simpler Hamiltonian $H_{\text{SU}(4)}$ based upon Wigner's SU(4) symmetry for protons and neutrons [24]. This Hamiltonian is computationally inexpensive and is used as a low-energy filter before starting the main calculation. This technique is described in Ref. [23].

In Table I we present lattice results for the ground state energies of ${}^4\text{He}$ and ${}^8\text{Be}$ up to NNLO. The method of calculation is nearly the same as that described in Ref. [13, 22, 25]. The higher-order corrections are computed using perturbation theory. The coefficients of the nucleon-nucleon interactions are set by fitting to low-energy scattering data. In our calculations the NNLO corrections correspond with three-nucleon forces. A detailed description of the interactions at each order can be found in Ref. [25]. We have used the triton binding energy and the weak axial vector current to fix the low-energy constants c_D and c_E entering the three-nucleon interaction.

In comparison with the calculations in Ref. [13], some improvements have been made using higher-derivative lattice operators which eliminate the overbinding of the leading order action when calculating larger nuclei such as ${}^{16}\text{O}$. The details of this improved action will be discussed in a forthcoming publication. The error bars in Table I are one standard deviation estimates which include both Monte Carlo statistical errors and uncertainties due to extrapolation at large Euclidean time. We see that the binding energy results for ${}^4\text{He}$ and ${}^8\text{Be}$ at NNLO are in agreement with experimental values.

In our projection Monte Carlo calculations we use a larger class of initial and final states than considered in previous work. For the calculation of ${}^4\text{He}$ we use an initial state with four nucleons, each at zero momentum. For the calculation of ${}^8\text{Be}$ we use the same initial state as ${}^4\text{He}$, but then apply creation operators after the first

TABLE I: Lattice results and experimental values for the ground state energies of ${}^4\text{He}$ and ${}^8\text{Be}$. All energies are in units of MeV.

	${}^4\text{He}$	${}^8\text{Be}$
LO [$O(Q^0)$]	-28.0(3)	-57(2)
NLO [$O(Q^2)$]	-24.9(5)	-47(2)
NNLO [$O(Q^3)$]	-28.3(6)	-55(2)
Experiment	-28.30	-56.50

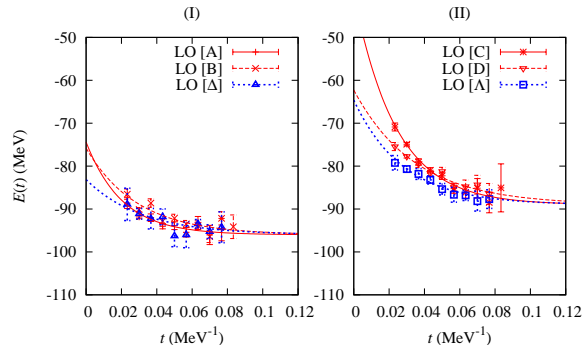


FIG. 1: Lattice results for the ${}^{12}\text{C}$ spectrum at leading order. In Panel I we show results from three different initial states, A, B, and Δ , each approaching the ground state energy. In Panel II we show results starting from three other initial states, C, D, and Λ . These trace out an intermediate plateau at energy about 7 MeV above the ground state.

time step to inject four more nucleons at zero momentum. The analogous process is done to extract four nucleons before the last step. This injection and extraction process of nucleons at zero momentum helps to eliminate directional biases caused by initial and final state momenta.

We make use of many different initial and final states to probe the structure of the ${}^{12}\text{C}$ states. In all of the ${}^{12}\text{C}$ states investigated here we measure four-nucleon correlations by calculating the expectation value of ρ^4 , where ρ is the total nucleon density. We find strong four-nucleon correlations consistent with the formation of alpha clusters. In Fig. 1 we present lattice results for the energy of ${}^{12}\text{C}$ at leading order versus Euclidean projection time t . For each of the initial states A, B, C, and D, we start with delocalized nucleon standing waves and use a strong attractive interaction in $H_{\text{SU}(4)}$ to allow the nucleons to self-organize into a nucleus. For initial states Δ and Λ , we use alpha cluster wavefunctions to recover the same states found using initial states A, B, C, and D. For these calculations, the interaction in $H_{\text{SU}(4)}$ is not as strong and the projected states retain their original alpha cluster character.

In Panel I, we show results from three different initial states, A, B, and Δ , each approaching the ground state

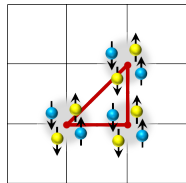


FIG. 2: This shows initial state Δ , a wavefunction consisting of three alpha clusters formed by Gaussian packets centered on the vertices of a compact triangle. There are a total of 12 equivalent orientations of this configuration.

energy, $-96(2)$ MeV. For initial state A, we start with four nucleons each at zero momentum, apply creation operators after the first time step to inject four more nucleons at rest, and then inject four more nucleons at rest after the second time step. The reverse process is used to extract nucleons for final state A. The same scheme is used for initial state B, though the interactions in $H_{\text{SU}(4)}$ used are not as strongly attractive as those for A.

For initial state Δ , we use a wavefunction consisting of three alpha clusters as shown in Fig. 2. The alpha clusters are formed by Gaussian packets centered on the vertices of a compact triangle. In order to construct eigenstates of total momentum and lattice cubic rotations, we consider all possible translations and rotations of the initial state. There are a total of 12 equivalent orientations of this configuration. We do not find fast convergence to the ground state when starting from any other configuration of alpha clusters. From this we conclude that the alpha cluster configurations in Fig. 2 have the strongest overlap with the 0_1^+ ground state of ^{12}C . The fact that it is an isosceles right triangle rather than an equilateral triangle is just an artifact of the lattice spacing.

In Panel II of Fig. 1 we show leading-order energies for three different initial states, C, D, and A, each approaching an intermediate plateau at $-89(2)$ MeV. If Euclidean time is taken to infinity, these curves eventually approach the ground state energy like the curves in Panel I. However it is clear that a different state is first being formed which is not the ground state. We identify the 0^+ state in this plateau region as the 0_2^+ Hoyle state. The common thread connecting each of the initial states C, D, and A, is that each produces a state which has an extended or prolate geometry. This is in contrast to the oblate triangular configuration in Fig. 2.

For initial state C, we take four nucleons at rest, four with momenta $(2\pi/L, 2\pi/L, 2\pi/L)$, and four with momenta $(-2\pi/L, -2\pi/L, -2\pi/L)$. For initial state D, we use a similar configuration with four at rest, four with momenta $(2\pi/L, 2\pi/L, 0)$, and four with momenta $(-2\pi/L, -2\pi/L, 0)$. For initial state A, we use a set three alpha clusters formed by Gaussian packets centered on the vertices of a bent-arm or obtuse triangular con-

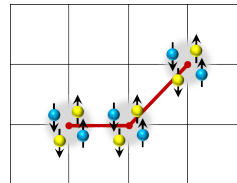


FIG. 3: This shows initial state Λ , a wavefunction consisting of three alpha clusters formed by Gaussian packets centered on the vertices of a bent-arm or obtuse triangular configuration. There are a total of 24 equivalent orientations of this configuration.

TABLE II: Lattice results for the low-lying even-parity states of ^{12}C compared with the experimental results in units of MeV.

	0_1^+	$2_1^+(E^+)$	0_2^+	$2_2^+(E^+)$
LO [$O(Q^0)$]	$-96(2)$	$-94(2)$	$-89(2)$	$-88(2)$
NLO [$O(Q^2)$]	$-77(3)$	$-74(3)$	$-72(3)$	$-70(3)$
NNLO [$O(Q^3)$]	$-92(3)$	$-89(3)$	$-85(3)$	$-83(3)$
Experiment	-92.16	-87.72	-84.51	$-82.6(1)$ [8, 10] $-82.32(6)$ [11] $-81.1(3)$ [9]

figuration as shown in Fig. 3. There are a total of 24 equivalent orientations of this configuration. We do not find the same plateau starting from other configurations of alpha clusters. We conclude that the configurations in Fig. 3 have the strongest overlap with the 0_2^+ Hoyle state of ^{12}C .

We use the same multi-channel method developed in Ref. [13] to find a spin-2 excitation above the ground state as well as a spin-2 excitation above the Hoyle state. In both cases we are taking the E^+ representation of the cubic rotation group on the lattice. We show the results for the binding energies of the low-lying even-parity states of ^{12}C in Table II. We find that the binding energies at NNLO are in agreement with experimental values.

In Table III we present results at leading order for the root-mean-square charge radius and quadrupole moment of the even-parity states of ^{12}C . We also show experimental values where available. In this study we compute electromagnetic moments only at leading order. We note that moments such as the charge radius for resonances above threshold are dependent on boundary conditions used to regulate the continuum-state asymptotics of the wavefunction. We avoid this problem because all of the low-lying states are bound at leading order. One expects that as the higher-order corrections push the binding energies closer to the triple alpha threshold, the corresponding radii will increase accordingly. A detailed study of these resonances as a function of finite volume size will be investigated in future work. We find good agreement with the experimental value for the 2_1^+ quadrupole moment. The difference in signs for the electric quadrupole

TABLE III: Lattice results at leading order and experimental values for the root-mean-square charge radius and the quadrupole moments for ^{12}C .

	LO	Experiment
$r(0_1^+)$ [fm]	2.2(2)	2.47(2) [26]
$r(2_1^+)$ [fm]	2.2(2)	–
$Q(2_1^+)$ [$e\text{ fm}^2$]	6(2)	6(3) [27]
$r(0_2^+)$ [fm]	2.4(2)	–
$r(2_2^+)$ [fm]	2.4(2)	–
$Q(2_2^+)$ [$e\text{ fm}^2$]	-7(2)	–

TABLE IV: Lattice results at leading order and experimental values for electromagnetic transitions involving the even-parity states of ^{12}C .

	LO	Experiment
$B(E2, 2_1^+ \rightarrow 0_1^+)$ [$e^2\text{ fm}^4$]	5(2)	7.6(4) [29]
$B(E2, 2_1^+ \rightarrow 0_2^+)$ [$e^2\text{ fm}^4$]	1.5(7)	2.6(4) [29]
$B(E2, 2_2^+ \rightarrow 0_1^+)$ [$e^2\text{ fm}^4$]	2(1)	–
$B(E2, 2_2^+ \rightarrow 0_2^+)$ [$e^2\text{ fm}^4$]	6(2)	–
$m(E0, 0_2^+ \rightarrow 0_1^+)$ [$e\text{ fm}^2$]	3(1)	5.5(1) [17]

moments of the two spin-2 states reflects the oblate shape of the 2_1^+ state and prolate shape of the 2_2^+ state.

The leading order results for the electromagnetic transitions among the even-parity states of ^{12}C are shown in Table IV. The definitions for these quantities can be found in Ref. [28]. The agreement with available experimental values is reasonable. The lattice results at leading order have a tendency to be somewhat smaller than experimental values. This presumably reflects the greater binding energies and smaller radii of the nuclei at leading order. We also predict electromagnetic decays involving the 2_2^+ state that may be measured experimentally in the near future.

In summary we have presented *ab initio* lattice calculations which show the structure of the Hoyle state and find evidence for a low-lying spin-2 rotational excitation. For the ground state and first spin-2 state, we find mostly a compact triangular configuration of alpha clusters. For the Hoyle state and second spin-2 state, we find a bent-arm or obtuse triangular configuration of alpha clusters. We have calculated charge radii, quadrupole moments, and electromagnetic transitions among the low-lying even-parity states of ^{12}C at leading order. All of the results are in reasonable agreement with experimental values. More work is still needed such as calculations using smaller lattice spacings. However these results provide a deeper understanding of the structure and rotations of the Hoyle state starting from first principles.

Acknowledgements We thank W. Nazarewicz, T. Neff, G. Rupak, H. Weller, and W. Zimmerman for useful discus-

sions. Partial financial support from the DFG and NSFC (CRC 110), HGF (VH-VI-417), BMBF (06BN7008) USDOE (DE-FG02-03ER41260), EU HadronPhysics3 project “Study of strongly interacting matter”, and ERC project 259218 NUCLEAREFT. Computational resources were provided by the Jülich Supercomputing Centre at the Forschungszentrum Jülich.

-
- [1] E. J. Öpik, Proc. Roy. Irish Acad. **A54**, 49 (1951).
 - [2] E. E. Salpeter, Astrophys. J. **115**, 326 (1952).
 - [3] E. E. Salpeter, Ann. Rev. Nucl. Sci. **2**, 41 (1953).
 - [4] F. Hoyle, Astrophys. J. Suppl. **1**, 121 (1954).
 - [5] C. Cook, W. A. Fowler, C. C. Lauritsen, and T. Lauritsen, Phys. Rev. **107**, 508 (1957).
 - [6] H. Morinaga, Phys. Rev. **101**, 254 (1956).
 - [7] A. Tohsaki, H. Horiuchi, P. Schuck, and G. Ropke, Phys. Rev. Lett. **87**, 192501 (2001).
 - [8] M. Freer et al., Phys. Rev. C **80**, 041303 (2009).
 - [9] S. Hyldegaard et al., Phys. Rev. C **81**, 024303 (2010).
 - [10] W. R. Zimmerman, N. E. Destefano, M. Freer, M. Gai, and F. D. Smit, Phys. Rev. C **84**, 027304 (2011).
 - [11] M. Itoh et al., Phys. Rev. C **84**, 054308 (2011).
 - [12] F. Smit, F. Nemulodi, Z. Buthelezi, J. Carter, R. Fearick, et al. (2012), 1206.4217.
 - [13] E. Epelbaum, H. Krebs, D. Lee, and U.-G. Meißner, Phys. Rev. Lett. **106**, 192501 (2011).
 - [14] R. Roth, J. Langhammer, A. Calci, S. Binder, and P. Navratil, Phys.Rev.Lett. **107**, 072501 (2011), 1105.3173.
 - [15] C. Forssen, R. Roth, and P. Navratil (2011), 1110.0634.
 - [16] M. Chernykh, H. Feldmeier, T. Neff, P. von Neumann-Cosel, and A. Richter, Phys. Rev. Lett. **98**, 032501 (2007).
 - [17] M. Chernykh, H. Feldmeier, T. Neff, P. von Neumann-Cosel, and A. Richter, Phys. Rev. Lett. **105**, 022501 (2010), 1004.3877.
 - [18] E. Epelbaum, H.-W. Hammer, and U.-G. Meißner, Rev. Mod. Phys. **81**, 1773 (2009).
 - [19] H. M. Müller, S. E. Koonin, R. Seki, and U. van Kolck, Phys. Rev. **C61**, 044320 (2000).
 - [20] D. Lee, B. Borasoy, and T. Schäfer, Phys. Rev. **C70**, 014007 (2004).
 - [21] E. Epelbaum, H. Krebs, D. Lee, and U. G. Meißner, Eur. Phys. J. **A41**, 125 (2009).
 - [22] E. Epelbaum, H. Krebs, D. Lee, and U.-G. Meißner, Phys. Rev. Lett. **104**, 142501 (2010).
 - [23] D. Lee, Prog. Part. Nucl. Phys. **63**, 117 (2009).
 - [24] E. Wigner, Phys. Rev. **51**, 106 (1937).
 - [25] E. Epelbaum, H. Krebs, D. Lee, and U.-G. Meißner, Eur. Phys. J. **A45**, 335 (2010).
 - [26] L. A. Schaller, L. Schellenberg, T. Q. Phan, G. Piller, A. Ruetschi, and H. Schnewly, Nucl. Phys. **A379**, 523 (1982).
 - [27] W. J. Vermeer et al., Phys. Lett. **B122**, 23 (1983).
 - [28] A. Bohr and B. R. Mottelson, *Nuclear Structure. Volume I: Single-Particle Motion* (W. A. Benjamin, New York, 1969).
 - [29] F. Ajzenberg-Selove, Nucl. Phys. **B506**, 1 (1990).